Influence of Internal Capsid Pressure on Viral Infection by Phage λ

Sarah Köster,[†‡§] Alex Evilevitch,[¶] Meerim Jeembaeva,[¶] and David A. Weitz[†‡*]
[†]Department of Physics and [‡]School of Engineering and Applied Sciences, Harvard University, Cambridge, Massachusetts; [§]Courant Research Centre Nano-Spectroscopy and X-Ray Imaging, University of Göttingen, Göttingen, Germany; and [¶]Department of Biochemistry, Center for Molecular Protein Science, Lund University, Lund, Sweden

ABSTRACT Ejection of the genome from the virus, phage λ, is the initial step in the infection of its host bacterium. In vitro, the ejection depends sensitively on internal pressure within the virus capsid; however, the in vivo effect of internal pressure on infection of bacteria is unknown. Here, we use microfluidics to monitor individual cells and determine the temporal distribution of lysis due to infection as the capsid pressure is varied. The lysis probability decreases markedly with decreased capsid pressure. Of interest, the average lysis times remain the same but the distribution is broadened as the pressure is lowered.

INTRODUCTION

Phage λ is an important and widely used model system for viruses that infect bacteria. It is also important and widely used in biotechnology, where it serves as both a platform for phage display and a vector for cloning recombinant DNA. The genome of phage λ is double-stranded DNA ~17 μm in length. To infect its host, *Escherichia coli*, the genome must be injected into the bacterium, leaving behind the protein capsid. However, the mechanism for this injection into the cytoplasm is still not fully understood. Entry into the cell requires the DNA to overcome a cytoplasmic pressure of at least 3×10^2 kPa, corresponding to an astonishingly high value of 3 atmospheres (1). However, the pressure inside the phage capsid, which is caused by the strong bending of the DNA and the repulsive forces between neighboring negatively charged chains, is considerably higher, on the order of 5×10^3 kPa (2). Indeed, in vitro experiments confirm that it is this internal capsid pressure that drives the DNA out of the phage capsid (2). Presumably, the same internal pressure is also responsible for driving the DNA into the cytoplasm of the host bacterium; however, there is no direct means to verify this assumption for the in vivo case. Bulk experiments, with mixtures of cells and phage in solution, can probe the evolution of cell and phage concentrations resulting from the infection. Although such studies provide important information about the competition between cells and phage, these ''classic'' multicell experiments are restricted to ensemble averaging over populations. For example, conditions for a stable equilibrium between phage and bacteria populations have been established (3,4). However, these experiments cannot access information on the level of single cells, which provides the most direct measure of the probability of infection; in particular, the dependence of the infection probability on the internal pressure cannot be investigated. Instead, experiments on individual cells are required. Such experiments must determine the time-dependent behavior of a population of individual cells. However, experimental probes at this level are difficult to realize and very rare.

Here we study the infection by phage λ of individual *E. coli* cells confined in isolated environments with volumes of a few picoliters. We vary the pressure within the capsids by using phage genomes of different lengths, and by changing the solution salt concentration. We find that the probability of cell lysis decreases with decreasing pressure inside the phage capsid. Control experiments confirm that lysis results from cell infection. Therefore, our results indicate a correlation between internal pressure and efficiency of in vivo phage infection.

MATERIALS AND METHODS

To isolate individual cells, we encapsulate bacteria in aqueous drops suspended in an inert oil using a microfluidic chip fabricated via soft lithography from poly(dimethylsiloxane) (PDMS). A schematic of the microfluidics device is shown in Fig. 1. The fluid connections are indicated by the circular regions. The drops are made in a flow-focusing geometry (5) shown in the magnified inset on the upper right. Drops containing cells are trapped for further study in the array of circular enclosures at the bottom of the schematic (6); a magnified view of these is shown at the bottom right. The drops can be easily loaded into this array as they are constrained within the circular traps by their surface tension; this prevents them from moving through the constrictions that connect the traps together. We use 8-pL drops that are flattened to a height of 10 μm by the depth of the channels; this leads to a drop diameter of 40 μm, ensuring that the full drop remains in the field of view of the microscope used to monitor the bacteria. The drops contain liquid broth medium (LB, Sigma, St. Louis, MO) to provide the cells with the usual nutrient environment (7), and a PFPE-PEG-block-copolymer surfactant (RainDance Technologies, Lexington, MA) prevents the drops from coalescing (9). *E. coli* MC4100 cells are grown in LB overnight to obtain a saturated culture at a concentration of 2.25×10^9 cells/mL.

Bacteriophages λ cI857 with genome lengths of 48.5 kbp (wild-type (WT)) and a shorter DNA mutant phage (b211) with a 37.7 kbp genome are produced by thermal induction of lysogenic *E. coli* strains. To increase the yield of phage induced in the cell, the strains are modified to grow without LamB protein expressed on their surface. The culture is then lysed by a temperature shift from 30°C to 42°C in a shaking water bath. The phage

Submitted May 11, 2009, and accepted for publication July 1, 2009.

*Correspondence: weitz@seas.harvard.edu

Alex Evilevitch's present address is Department of Physics, Carnegie Mellon University, Pittsburgh, Pennsylvania.

Editor: Denis Wirtz.

0006-3495/09/09/1525/5 $2.00

doi: 10.1016/j.bpj.2009.07.007

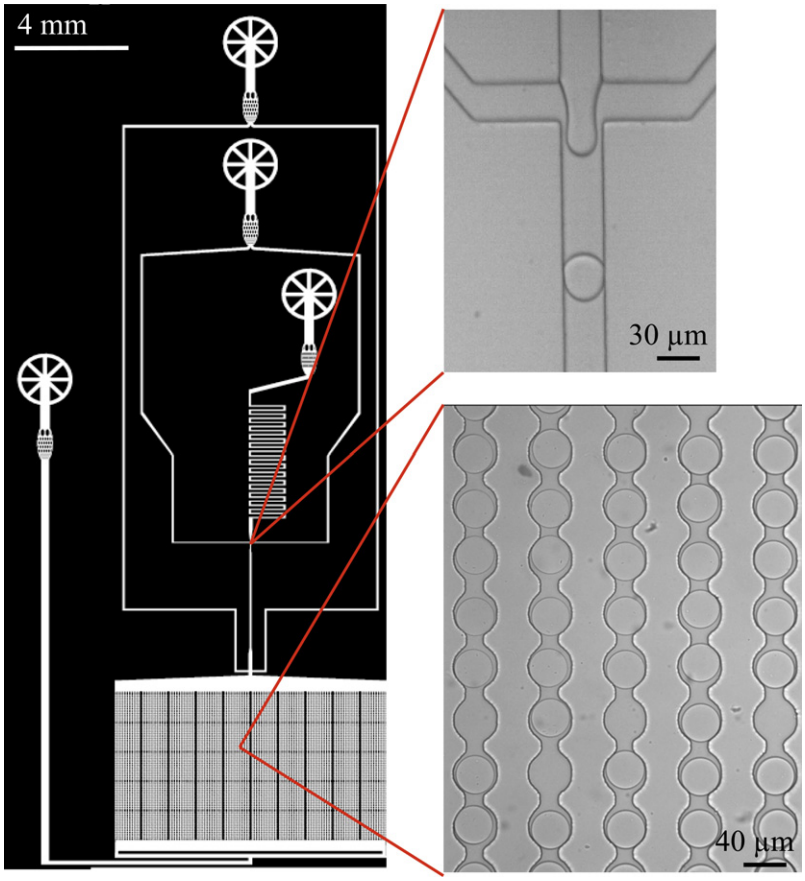

FIGURE 1 Microfluidics device used in the experiments. A micrograph of the drop production site is shown on the upper right, and a micrograph of the trapping region is shown on the bottom right.

samples are purified by CsCl equilibrium centrifugation. The samples are dialyzed from CsCl against TM buffer (50 mM Tris-HCl, pH 7.4, and 10 mM MgSO4). The final titer is 1.5×10^{11} virions/mL, as determined by plaque assay. These phages have a temperature-sensitive repressor that restricts them to the lytic cycle at 37°C, which is the temperature of optimal growth of the host bacterium. The lysogenic cycle, in which latent phage DNA is present within the cell, is suppressed at 37°C, the temperature used in these experiments. Thus these phages are well suited for the study of cell lysis due to phage infection.

To confirm the adsorption of the phage λ on the *E. coli*, we fluorescently label the virus DNA with SYBR gold in a bulk experiment. A micrograph of a bulk sample of fluorescently labeled phage is shown in Fig. 2 *a*. Upon addition of *E. coli*, the phage adsorbs to the cells, as demonstrated by a comparison of the bright-field image showing the location of the cells (Fig. 2 *b*), and the corresponding fluorescence image showing the location of the phage (Fig. 2 *c*).

For the microfluidics experiments, we mix cells and phage at ~7 viruses per bacterium in the presence of 20 mM $MgSO_4$, and incubate and shake the mixture in an open tube at 30°C to allow the phage to adsorb to the cells. We estimate the diffusion-limited time for encounter between a phage and a bacterium to be 100 s; therefore, we incubate for 15 min before quenching further adsorption of phage by dilution with LB to a final concentration of 1.13×10^8 cells/mL. We adjust the suspension to a final concentration of 10 mM $MgSO_4$ and incubate at 37°C for 60 min. This procedure ensures that the cells have time to overcome their lag phase before they enter their exponential growth phase, where we study the bacterial susceptibility to phage infection. The relative phage concentration is chosen to ensure that neither species becomes extinct in a bulk experiment in which oscillatory growth for the cell and phage populations occurs instead (3,10). These oscillations reflect the dynamics of the interactions between the bacteria and virus. When the bacteria population dominates, the virus population can infect numerous individual cells; as a result, the viruses replicate faster, increasing their population. However, this increase is ultimately limited by the availability of bacteria cells, and thus does not persist; instead, the bacterial population again increases and the cycle starts anew. These conditions are adjusted to optimize the experiments on the microfluidics device. We image the drops at one frame per minute over 4 h using a 20× objective,

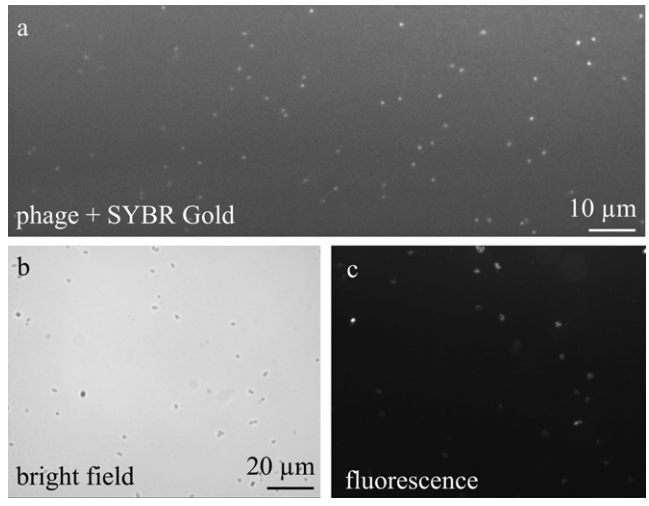

FIGURE 2 (*a*) Micrograph of a bulk sample of fluorescently labeled phage. (*b* and *c*) After addition of *E. coli*. Compare the (*b*) bright-field image showing the location of the cells, and (*c*) the fluorescence image showing the location of the phage.

enabling us to simultaneously monitor 40 drops, which contain ~70 cells in total.

RESULTS AND DISCUSSION

To ensure the compatibility of the microfluidics (7,9), we confirm that the *E. coli* growth in droplets is similar to that in bulk culture in the absence of phage; the initial doubling times, as well as the saturation concentration, are both comparable. Of interest, however, the cells grow into long chains or tighter bunches, and daughter cells do not always break off after cell division (for typical examples, see Fig. 3 *a* and Movie S1, Movie S2, Movie S3, and Movie S4 in the Supporting Material). This may result from environmental or confinement effects; however, similar growth structures are observed for a closely related strain after it develops a resistance to phage (11).

Upon addition of phage λ, we observe three distinct classes of cell behavior. The largest group of cells is unaffected and continues to grow, and the behavior is indistinguishable from that of the cells in the drops in the absence of phage, as shown in Fig. 3 *b*. Surprisingly, we also find a group of cells that remain in the drops as single cells with no sign whatsoever of proliferation; an example is shown in Fig. 3 *c*. These cells are clearly affected by the virus, since we never observe such behavior in the absence of phage. Nevertheless, the phage is apparently not able to replicate and lyse the cell in a normal fashion. This group of cells must be included in any model describing the infection processes if the interaction between phage and its host is to be fully understood. These cells cannot be observed in traditional bulk experiments, but we nevertheless expect that they do affect the interplay of cell growth and virus replication and the relative numbers in each population. However, although the exact origin of this behavior is unclear, this population of cells has no effect on our conclusions. Finally, there are also a considerable number of cells that are lysed by the phage, and we can precisely measure the time of their disappearance, as indicated in Fig. 3 *d*. This enables us to study cell lysis caused by phage infection on a single-cell level for many cells simultaneously. We show the relative probabilities for the fate of the cells in the presence of WT phage in Fig. 4.

To investigate the role of internal pressure within the WT phage capsid, we add 1 mM of spermine-tetrahydrochloride to the solution after the initial 15-min incubation step during which phage adsorption occurs. Spermine is a tetravalent polyamine cation and should introduce an attractive interaction that promotes DNA condensation and compaction (12), thereby reducing the self-repulsion of the highly bent, negatively charged DNA, which in turn reduces the internal pressure (2). As a control, we ensure that the additional salt does not affect normal bacteria growth in separate cell-culture experiments. Upon addition of the spermine, we observe a decrease in infection probability from 31% to 24%, as shown in Fig. 4, and a concomitant increase in the fraction of growing cells from 48% to 57%. In vitro experiments show that only 40% of the genome is ejected in the presence of 1 mM spermine, provided that DNase is added to digest the ejected DNA (13). By analogy, we hypothesize that in vivo, the decreased internal pressure caused by the reduced DNA-DNA repulsion may be at least partially responsible for the decreased infection probability (14).

Although a spermine-induced reduction of the internal pressure is an appealing explanation for the decrease in infection probability, the difference is not significant ($p > 0.05$); moreover, spermine can also affect the transmembrane potential of the cell, which may have an effect on infection. Thus,

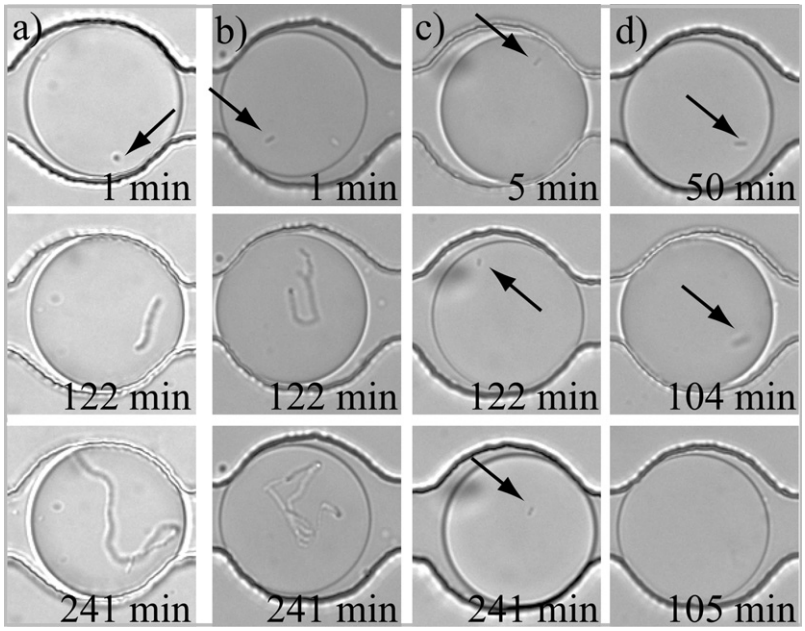

FIGURE 3 (*a*) Control with no phage present in the drop; cell growth. (*b–d*) Phage present in the drops. (*b*) Cell growth. (*c*) Cell remains without proliferation. (*d*) Cell lysis. See Movie S1, Movie S2, Movie S3, and Movie S4.

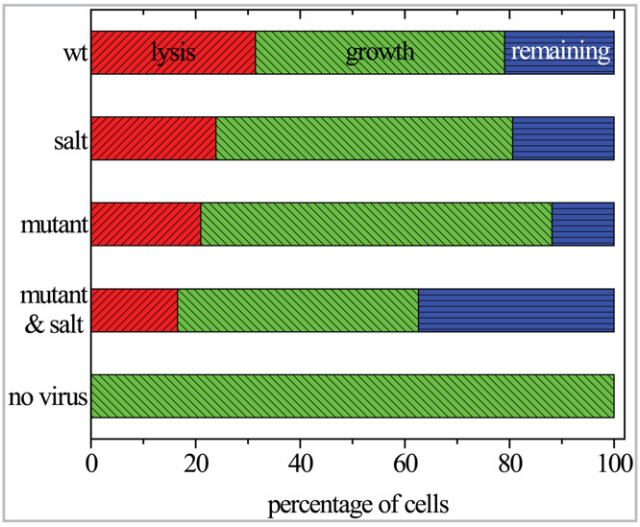

FIGURE 4 Probability that cells will be infected by bacteriophage for different parameters. Parameters that decrease the pressure in the phage capsid also decrease the probability for infection. When the pressure is lowered by decreasing the genome length, the difference becomes significant ($p < 0.05$).

a more compelling test of our hypothesis would be to directly decrease the pressure within the capsid independently of the salt concentration. We accomplish this by using the λ-mutant b221 (cI857), which has a shorter genome length of only 37.7 kbp (15) corresponding to ~78% of the 48.5-kbp-long WT genome. This results in a decrease in capsid pressure from 250 kPa to 150 kPa in Tris buffer, as measured by in vitro experiments that include both the virus and the receptor that triggers the genome release (16); however, the packing efficiency of the DNA into phage capsids during replication remains essentially constant (17) since this reduction in genome length is still within the limit for efficient packing (18). For shorter genomes, the packing efficiency of the genome in the capsid decreases dramatically, and we refrain from using such genomes in our study. By selecting the b221 deletion, which does not take out any particular gene or function crucial for packaging (17) and lytic growth (19), we ensure that the infectivity of the phage will not be modified. Furthermore, the same deletion is made when λ-phage is used for cloning purposes. Other DNA inserts are then introduced into this deletion region in λ-chromosome without affecting the efficiency of in vivo infectivity of phage particles (20). Moreover, structurally, no differences are observed between this deletion mutant and WT phage (21). Thus, differences in the probability for a cell to become lysed should result from differences in infection probability; these in turn should reflect the effects of the modified internal capsid pressure. The infection probability for the short genome is indeed decreased significantly ($p = 0.038$) to 21% from 31% for the long genome, as shown in Fig. 4. At the same time, the percentage of cells that show growth in the drops is increased from 48% to 67% with decreased genome length. Thus, a pressure drop of 40% leads to a decrease in infection probability by 30%. These results support our hypothesis that a lower capsid pressure leads to a lower probability of cell infection. The deletion of a part of the genome could potentially also impair one of the many steps of the viral cycle, which could lead to lower infection probability. However, the combined results from complementary experiments with added salt and those with a shorter genome phage mutant, as well as the parallelism to in vitro experiments employing mutant phage (16), suggest that the lowered capsid pressure is most likely responsible for the decreased probability of infection.

Since changing either the DNA length or the DNA-DNA interaction leads to a decreased infection probability, we also investigate the consequences of both effects by adding 1 mM spermine to the phage with the shorter genome length. Presumably, both effects are independent and thus should decrease the internal capsid pressure in an additive manner. Our results show that this is indeed the case: The infection probability decreases to 17%, corresponding to a 50% reduction from the WT phage in the absence of spermine; this decrease is highly significant ($p = 0.003$). However, we also observe an increased number of cells that remain but do not proliferate by comparison to the other experiments. The origin of this behavior is unclear and requires further investigation.

To help elucidate the origin of the dependence of phage infection on the pressure inside the capsid, we investigate the time dependence of lysis. Our measurements provide data from individual cells and thus allow us to determine the full distribution of lysis times; this is a unique feature of this microfluidic approach. We focus on the variation of pressure with genome length since it is the most direct way of varying pressure in the capsid and is independent of the trafficking of salt ions into the capsid. We compare the distribution for the WT phage with that of the mutant with the shorter genome and fit the data to Gaussians, as shown in Fig. 5; surprisingly, we find that the average time for lysis is virtually unaffected by the genome length. We obtain 189 ± 1 min for the WT genome compared to 178 ± 5 min for the short genome; these lysis times are comparable to those measured in bulk samples (22). By contrast, the width of the distribution for the short-genome phage is considerably larger (by a factor of ~3.5) than that for the WT genome.

The markedly wider distribution of lysis times for the shorter genome phage suggests that some cells are lysed much earlier than with WT phage, whereas other cells are lysed much later. This may reflect two competing effects: The long-time tail in the distribution may reflect the effects of the lower internal pressure within the capsid of the mutant phage, which decreases the likelihood of DNA entering the cell, thereby delaying phage infection and subsequent lysis for some cells. However, once the DNA is injected into the cell, transcription of the shorter genome will be faster, resulting in more rapid replication of the phage. Thus, the

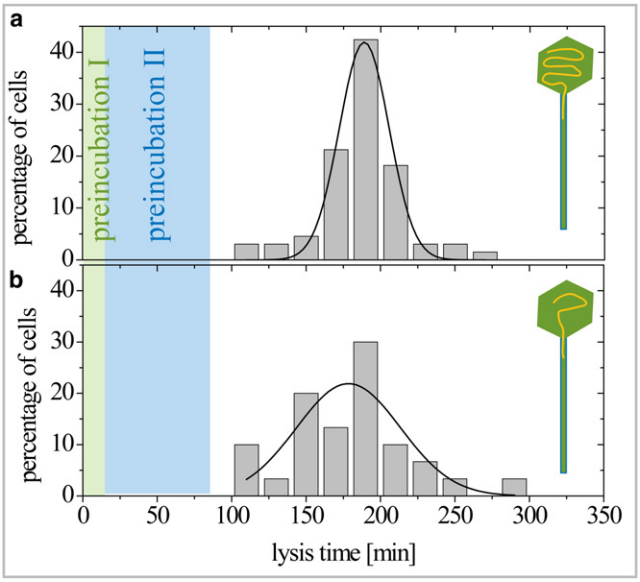

FIGURE 5 Time distribution for cell lysis after infection for (*a*) WT λ-DNA (48.5 kbp) and (*b*) short λ-DNA (37.7 kbp).

short-time tail in the distribution may reflect lysis of those cells that are infected at early times. Alternatively, it is possible that the reduced osmotic pressure in the capsid is not sufficient to inject the full genome into the cell, resulting in incomplete expression of the full suite of genes. This may also result in differences in the infection rate, which is reflected by the modified distribution of lysis times.

The unique ability to study phage infection on the single-cell level provides important new information that helps elucidate the effect of internal pressure within the phage capsid on the infection mechanism. This technique can easily be adapted for measurements on animal and human viruses to provide new insights into the infection mechanisms. Furthermore, an enormous parameter space, which currently can only be explored by computer simulations, becomes experimentally accessible with this method. For example, the effects of varying incubation times and cell concentration, number of viruses per cell, or valence of added salt can all be explored. This should significantly improve our understanding of the infection mechanisms.

SUPPORTING MATERIAL

Four movies are available at http://www.biophysj.org/biophysj/supplemental/S0006-3495(09)01227-2.

We thank Christian Schmitz, Michael Brenner, Richard Losick, and Thomas Silhavy for fruitful discussions, and RainDance Technologies for providing the surfactant. We are grateful to Michael Feiss for valuable advice and for critically reading our manuscript, and to Georg Grön and Oliver Adolph for their help with the statistical analysis.

This work was supported by the National Science Foundation (DMR-0602684 and DBI-0649865), the Harvard Materials Research Science and Engineering Center (DMR-0820484), and the Human Frontier in Science Program (RGP0004/2005-C102). S.K. was supported by the Deutsche Forschungsgemeinschaft (KO 3572/1) and funded by the German Excellence Initiative.

REFERENCES

1. Neidhardt, F. 1996. *Echerichia coli* and *Salmonella typhimurium*. ASM Press, Washington, DC.
2. Evilevitch, A., L. Lavelle, C. M. Knobler, E. Raspaud, and W. M. Gelbart. 2003. Osmotic pressure inhibition of DNA ejection from phage. *Proc. Natl. Acad. Sci. USA*. 100:9292–9295.
3. Levin, B. R., F. M. Stewart, and L. Chao. 1977. Resource-limited growth, competition, and predation: a model and experimental studies with bacteria and bacteriophage. *Am. Nat.* 111:3–24.
4. Horne, M. T. 1970. Coevolution of *Escherichia coli* and bacteriophages in chemostat culture. *Science*. 168:992–993.
5. Anna, S. L., N. Bontoux, and H. A. Stone. 2003. Formation of dispersions using "flow focusing" in microchannels. *Appl. Phys. Lett.* 82:364–366.
6. Schmitz, C. H. J., A. C. Rowat, S. Köster, and D. A. Weitz. 2009. Dropspots: a picoliter array in a microfluidic device. *Lab Chip*. 9:44–49.
7. Köster, S., F. E. Angile, H. Duan, J. J. Agresti, A. Wintner, et al. 2008. Drop-based microfluidic devices for encapsulation of single cells. *Lab Chip*. 8:1110–1115.
8. Reference deleted in proof.
9. Holtze, C., A. C. Rowat, J. J. Agresti, J. B. Hutchison, F. E. Angilè, et al. 2008. Biocompatible surfactants for water-in-fluorocarbon emulsions. *Lab Chip*. 8:1632–1639.
10. Beretta, E., and Y. Kuang. 1998. Modeling and analysis of a marine bacteriophage infection. *Math. Biosci.* 149:57–76.
11. Lacqua, A., O. Wanner, T. Colangelo, M. G. Martinotti, and P. Landini. 2006. Emergence of biofilm-forming subpopulations upon exposure of *Escherichia coli* to environmental bacteriophages. *Appl. Environ. Microbiol.* 72:956–959.
12. Bloomfield, V. A. 1997. DNA condensation by multivalent cations. *Biopolymers*. 44:269–282.
13. Evilevitch, A. 2006. Effects of condensing agent and nuclease on the extent of ejection from phage. *J. Phys. Chem. B*. 110:22261–22265.
14. Harrison, D. P., and V. C. Bode. 1975. Putrescine and certain polyamines can inhibit DNA injection from bacteriophage λ. *J. Mol. Biol.* 96:461–470.
15. Parkinson, J. S., and R. J. Huskey. 1971. Deletion mutants of bacteriophage λ. I. Isolation and initial characterization. *J. Mol. Biol.* 56: 369–384.
16. Grayson, P., A. Evilevitch, M. M. Inamdar, P. K. Purohit, W. M. Gelbart, et al. 2006. The effect of genome length on ejection forces in bacteriophage λ. *Virology*. 348:430–436.
17. Feiss, M., R. A. Fisher, M. A. Crayton, and C. Egner. 1977. Packaging of the bacteriophage λ chromosome: effect of chromosome length. *Virology*. 77:281–293.
18. Feiss, M., and D. A. Siegele. 1979. Packaging of the bacteriophage λ chromosome: dependence of cos cleavage on chromosome length. *Virology*. 92:190–200.
19. Hendrix, R., J. Roberts, F. Stahl, and R. Weisberg. 1983. Lambda II. Cold Spring Harbor Laboratory Press, Woodbury, NY.
20. Hohn, B., and K. Murray. 1977. Packaging recombinant DNA molecules into bacteriophage particles in vitro. *Proc. Natl. Acad. Sci. USA*. 74:3259–3263.
21. Ivanovska, I., G. Wuite, B. Jonsson, and A. Evilevitch. 2007. Internal DNA pressure modifies stability of WT phage. *Proc. Natl. Acad. Sci. USA*. 104:9603–9608.
22. Sambrook, J., and D. W. Russell. 2001. Molecular Cloning: A Laboratory Manual. Cold Spring Harbor Laboratory Press, Cold Spring Harbor, New York.